available at www.sciencedirect.com

ScienceDirect

journal homepage: www.elsevier.com/locate/biochempharm

Involvement of reactive oxygen species on the apoptotic mechanism induced by IFN-α2b in rat preneoplastic liver

Ariel D. Quiroga, María de Luján Alvarez, Juan P. Parody, María Teresa Ronco, Daniel E. Francés, Gerardo B. Pisani, Cristina E. Carnovale, María Cristina Carrillo *

Instituto de Fisiología Experimental, Consejo Nacional de Investigaciones Científicas y Técnicas (CONICET), Facultad de Ciencias Bioquímicas y Farmacéuticas, Universidad Nacional de Rosario, Rosario, Argentina

ARTICLE INFO

Article history:
Received 27 December 2006
Accepted 13 February 2007

Keywords:
Hepatocarcinogenesis
Apoptosis
Oxidative stress
Transforming growth factor-β_1
NADPH oxidase

JEL classification:
Gastrointestinal pharmacology

ABSTRACT

Interferon-α2b (IFN-α2b) is an important component in the preventive treatment of patients who have severe hepatic illness such as hepatitis B or C and hepatocarcinomas. In a previous work, using a rat liver preneoplastic model, we have demonstrated that IFN-α2b reduces the number and volume of altered hepatic foci (AHF) inducing apoptosis through a mechanism mediated by TGF-β_1. In this study, the implication of hepatocytes redox status of IFN-α2b-treated preneoplastic liver in the TGF-β_1-induced apoptotic death was analyzed. Results indicate that IFN-α2b induces hepatocytic TGF-β_1 production and secretion by induction of reactive oxygen species (ROS) formation through the activation of a membrane bound NADPH oxidase complex. TGF-β_1, in turn, reduces hepatocytes antioxidant defenses and induces programmed cell death. On the other hand, it was also demonstrated that treatment of rats with IFN-α2b plus a ROS scavenger such as ascorbic acid, abolishes the apoptotic effect of IFN-α2b in rat preneoplastic livers, leading to an increase of the foci volume. In conclusion, these findings strongly suggest that ROS have a fundamental role as signaling and/or regulator molecules in the IFN-α2b-induced apoptosis in hepatic preneoplastic cells.
© 2007 Elsevier Inc. All rights reserved.

1. Introduction

Several experimental studies have shown that interferon-α (IFN-α) exerts an antiproliferative effect against hepatocarcinoma cell lines by inducing apoptosis and inhibiting cell cycle progression [1,2]. Little is known concerning the *in vivo* action of IFN-α in the clinically undetectable very-early-stage of hepatocarcinogenesis. In this connection, results of our laboratory have demonstrated that IFN-α2b induces apoptosis of preneoplastic foci in rat livers [3] and this effect is mediated by transforming growth factor-β_1 (TGF-β_1) secreted by hepatocytes themselves under IFN-α2b induction [4].

Several lines of evidence indicate that TGF-β_1 induces reactive oxygen species (ROS) production, which initiate mitochondrial dysfunction and activation of the apoptotic machinery [5,6]. Source of ROS in the TGF-β_1-induced apoptosis is poorly known. It has been described that TGF-β_1 induces a NADPH oxidase system in fetal rat hepatocytes

* *Corresponding author at*: Instituto de Fisiología Experimental (IFISE), Facultad de Ciencias Bioquímicas y Farmacéuticas, Universidad Nacional de Rosario, Suipacha 570, 2000-Rosario, Argentina. Tel.: +54 341 4305799; fax: +54 341 4399473.
E-mail addresses: mcarrill@fbioyf.unr.edu.ar, carrillo@ifise.gov.ar (M.C. Carrillo).

Abbreviations: IFN-α2b, interferon alfa-2b; TGF-β_1, transforming growth factor-β_1; ROS, reactive oxygen species; SOD, superoxide dismutase; CAT, catalase; tGSH, total intracellular glutathione; GSSG, oxidize glutathione; IP, initiation-promotion; ASC, ascorbic acid; DPI, diphenyleneiodonium; RT-PCR, reverse transcription polymerase chain reaction; GCL, glutamate cysteine ligase; GAPDH, glyceraldehyde-3-phosphate dehydrogenase; DCFH-DA, 2′,7′-dichlorofluorescin diacetate; rGST P, placental form of rat glutathione S-transferase; AHF, altered hepatic foci; PI, proliferative index; PCNA, proliferating cell nuclear antigen; TUNEL, terminal deoxynucleotidyl transferase mediated biotin-deoxyuridine triphosphate nick-end labeling; AI, apoptotic index

0006-2952/$ – see front matter © 2007 Elsevier Inc. All rights reserved.
doi:10.1016/j.bcp.2007.02.007

[7]. NADPH oxidases are plasma-membrane associate enzymes that catalyze the production of superoxide from oxygen and NADPH and are the major candidates for the production of ROS in several cell types [8] including hepatocytes [9]. Besides, recent studies that characterize time-dependent changes in gene expression during TGF-β_1-induced apoptosis in hepatoma cells, have shown that genes encoding proteins involved in antioxidant defenses are downregulated, including superoxide dismutases (SODs), catalase (CAT), and enzymes of the glutathione synthesis pathway [10].

The present work was aimed to further analyze the intrinsic mechanism implied in the IFN-α2b-induced apoptotic process of hepatocytes from preneoplastic liver. We demonstrated that IFN-α2b produces an increase of ROS which, in turn, induces TGF-β_1 production and secretion. TGF-β_1 enhances ROS production and modifies the redox status of preneoplastic liver cells, initiating the apoptotic process.

These results suggest that the overexpression of ROS is beneficial for the apoptotic effect initiated by IFN-α2b. These findings provide novel understanding of the relationship of cytokines during the preneoplastic events.

2. Materials and methods

2.1. Reagents

Diethylnitrosamine (DEN), 2-acetylaminofluorene (2-AAF), collagenase, GSH, GSH reductase, ascorbic acid (ASC), diphenyleneiodonium (DPI), 2′,7′-dichlorofluorescin diacetate (DCFH-DA) and NADPH were from Sigma Chemical Co. (St. Louis, MO). Anti-rGST P antibody was provided by Immunotech (Marseille, France). Anti-TGF-β_1, anti-PCNA and anti-GCL antibodies were from Santa Cruz Biotechnology (Santa Cruz, CA). IFN-α2b was kindly provided from Bio Sidus S.A. (Buenos Aires, Argentina). ECL™ Western blotting analysis system was purchased from Amersham Pharmacia Biotech (Buckinghamshire, UK). All other chemicals were of the highest grade commercially available.

2.2. In vitro studies

2.2.1. Animals and treatment

Adult male Wistar rats weighing 330–380 g were maintained in a room at a constant temperature with a 12 h light–dark cycle, with food and water supplied *ad libitum*. All procedures described were performed according to the ''Guide for the Care and Use of Laboratory Animals'' (National Institutes of Health, publication no. 25–28, revised 1996). Rats were subjected to a 2-phase or initiation-promotion (IP) model of rat hepatocarcinogenesis [3]. Briefly, animals received 2 intraperitoneal necrogenic doses of DEN (150 mg/kg body weight) 2 weeks apart. One week after the last injection of DEN, the rats received 20 mg/kg body weight of 2-AAF by gavage for 4 consecutive days per week during 3 weeks. Animals were killed at the end of the sixth week.

2.2.2. Cell isolation and culture

Hepatocytes from preneoplastic rat livers were isolated by collagenase perfusion and mechanical disruption as previously described [12]. A hepatocyte-enriched population from the entire liver (containing both preneoplastic hepatocytes plus hepatocytes from the surrounding tissue) was obtained by centrifugation. Neither selective loss nor enrichment of preneoplastic cells occurred during cell isolation (data not shown). Hepatocytes were seeded in RPMI medium with L-glutamine supplemented with 10% fetal calf serum, penicillin (100 U/mL) and streptomycin (100 μg/mL). Hepatocytes were incubated at 37 °C in a humidified atmosphere of 95% O_2 and 5% CO_2 for 2 h, allowing cells attachment to plates. After that time, medium was changed to fresh RPMI medium supplemented with 0.2% fetal calf serum, penicillin (100 U/mL) and streptomycin (100 μg/mL). Hepatocytes were incubated at the times indicated in the figures, and treated with: (a) 10^5 U/mL IFN-α2b, (b) 10^5 U/mL IFN-α2b plus 0.04 μg/mL anti-TGF-β_1, (c) 10^5 U/mL IFN-α2b plus 1000 μM ASC, or (d) left untreated. Cells treated with anti-TGF-β_1, or ASC were used as controls. The dose of IFN-α2b used induced a similar increment in the apoptotic cell death to the one observed *in vivo*, when rats with preneoplasia received IFN-α2b at therapeutic doses [3].

The viability of all cell suspensions was checked with a Trypan Blue exclusion assay [6]. Hepatocytes suspensions with less than 85% of viability were discarded.

2.2.3. Secretion of TGF-β_1 to the culture media

Hepatocyte-conditioned media were collected at different times and TGF-β_1 was quantitated using an ELISA test (R&D Systems, Minneapolis, MN).

2.2.4. RNA isolation and RT-PCR

Total RNA was isolated using the TriZOL method (Life Technologies, Gaithersburg, MD). RNA was dissolved in RNAse-free water and kept at −80 °C until use. Reverse transcription of 3 μg of total RNA was performed with oligo-dT primer, and cDNA samples were stored at −20 °C until assayed. Conditions and the design of the primer sets (TIB Molbiol LLC, Adelphia, NJ) for the PCR reaction are given in Table 1. RT-PCR products were then resolved on a 1.5% agarose gel and bands were visualized using a high performance ultraviolet transilluminator (UVP, CA). Images of the RT-PCR ethidium bromide-stained agarose gels were acquired and quantification of the optical density (OD) of bands was performed using the Gel-Pro Analyzer (Media Cybernetics) software. Results were expressed as the ratio between the intensities of TGF-β_1 or the catalytic subunit of glutamate cysteine ligase (GCLC) ODs and glyceraldehyde-3-phosphate dehydrogenase (GAPDH) OD.

2.2.5. Measurement of apoptosis

Apoptosis was investigated using the FITC-Annexin V Apoptosis Kit (BD Biosciences, San Jose, CA). Cultured hepatocytes were stained following the manufacturer's protocol. Then cells were washed, fixed, and viewed under fluorescence microscope. Apoptotic cells were counted by examining >1000 cells/dish and expressed per 100 hepatocytes.

2.2.6. Measurement of intracellular ROS

Formation of ROS was determined as previously described [13], with slight modifications. Cells were loaded with 5 μM DCFH-DA for 20 min at 37 °C with 5% CO_2. Then, cells were washed, scrapped off and fluorescence was measured on a

Table 1 – Primers and PCR conditions

Substance		Primer sequences	Conditions
TGF-β_1			Thermal cycles: 35
	for	5′-GGACTACTACGCCAAAGAAG-3′	Denaturing phase: 95 °C—1 min
	rev	5′-TCAAAAGACAGCCACTCAGG-3′	Annealing phase: 54 °C—1 min
			Extension phase: 72 °C—1 min
GCLC			Thermal cycles: 32
	for	5′-CCTTCTGGCACAGCACGTTG-3′	Denaturing phase: 94 °C—30 s
	rev	5′-TAAGACGGCATCTCGCTCCT-3′	Annealing phase: 55 °C—30 s
			Extension phase: 72 °C—2 min
GAPDH			Thermal cycles: 30
	for	5′-CCACCCATGGCAAATTCCATGGCA-3′	Denaturing phase: 94 °C—45 s
	rev	5′-TCTAGACGGCAGGTCAGGTCAACC-3′	Annealing phase: 60 °C—45 s
			Extension phase: 72 °C—2 min

All reactions were followed by a final elongation step at 72 °C for 7 min.

Shimadzu Spectrofluorophotometer RF-5301 PC (excitation wavelength 488 nm, emission wavelength 525 nm).

2.2.7. *NADPH oxidase activity assay*

Cells were detached, pelleted and resuspended. NADPH oxidase activity was analyzed as previously described. Briefly, hepatocytes were incubated with 250 μM NADPH, and NADPH consumption was monitored by the decrease in absorbance at 340 nm for 10 min. The specific activity was analyzed by adding 10 μM DPI 30 min before the assays. The absorption extinction coefficient used to calculate the amount of NADPH consumed was 6.22 mM^{-1} cm^{-1} [7].

2.2.8. *GSH content and glutamate cysteine ligase (GCL) activity assays*

Cultured hepatocytes (10^6 per dish) were washed, sonicated and pelleted at 4 °C. Total glutathione (tGSH) content (GSH + GSSG) was determined by a modification of the Tietze assay [14]. In some experiments, culture media were also collected and glutathione content was analyzed in a similar manner.

For GCL activity measurements, pellets were washed before lysis to remove any traces of remaining cysteine from the media. GCL activity was determined as described previously by Seelig et al. [15].

2.2.9. *Antioxidant enzymes assays*

Hepatocytes were washed, sonicated and centrifuged. The supernatants were subjected to enzyme assays. CAT activity was determined by monitoring the rate of decomposition of H_2O_2, as a function of the decrease in absorbance at 240 nm [16]. SOD activity was assayed by a method based on the inhibition of nitrite formation from hydroxylammonium in the presence of superoxide anion generators, as previously described [17].

2.2.10. *Protein concentration determination*

The protein concentration was determined by Lowry method [18], using bovine serum albumin as a standard.

2.3. *In vivo studies*

2.3.1. *Animals and treatments*

Animals subjected to the 2-phase model of cancer development (see Section 2.2.1) were divided into four groups of 8 to 10 rats each: group 1 of IP rats; group 2 of IP rats that also received IFN-α2b 6.5 10^5 U/kg body weight, administered intraperitoneally 3 times per week (IP + IFN-α2b). The dose used was comparable to that used for therapeutic purposes [3]; group 3 of IP rats that received IFN-α2b and ASC, 75 mg/kg body weight, intraperitoneally 3 times per week [11] (IP + IFN-α2b + ASC); group 4 of IP rats that only received ASC (IP + ASC).

2.3.2. *Placental form of rat glutathione S-transferase (rGST P) positive cells analysis*

Liver slices from different lobes were fixed in 10% v/v formalin solution and embedded in low melting paraffin. Immunohistochemical staining was performed by the peroxidase–anti-peroxidase method [19], using the antibody raised against rGST P. Sections were counterstained with hematoxylin. Because this isozyme has been described as the most effective single marker of hepatic preneoplasia in the rat [20], immunohistochemical detection of rGST P is the most widely used method for identification, quantization and assessment of rat altered hepatic foci (AHF) [21]. A representative number of field sections (usually 1 to 1.5 cm^2 of tissue per animal was evaluated) from each group were collected using a CCD color video camera (Sony SSC-c370) attached to a Zeiss Axiolab microscope. Images were processed using a NIH imaging analysis system. The number of AHF per liver and AHF as percentage of liver were calculated according to the modified Saltykov method [22] by using the digitized images.

2.3.3. *Determination of proliferative index (PI)*

To investigate differences in proliferation activity in rGST P-positive foci among the experimental groups, consecutive section slides were examined by immunohistochemical staining with anti-rGST P and anti-proliferating cell nuclear antigen (PCNA) antibodies, determined by the method of Greenwell et al. [23].

2.3.4. *Determination of apoptotic index (AI)*

Quantitative analysis of apoptosis was performed by *in situ* specific labeling of fragmented DNA using a modified terminal deoxynucleotidyl transferase mediated biotin-deoxyuridine triphosphate nick-end labeling (TUNEL) method [24] (Promega, Madison, WI) in consecutive sections of those stained for rGST P. Apoptotic cells were counted in AHF (by scoring at least

1000–5000 preneoplastic hepatocytes) and surrounding hepatocytes (at least 5000–10000 hepatocyte nuclei were examined) only if they were TUNEL positive and displayed hallmark characteristics of apoptosis. AI was expressed as apoptotic cells scored per 100 hepatocytes. In order to corroborate the incidence of apoptotic bodies, serial sections were stained with hematoxylin/eosin.

2.4. *Statistical analysis*

The results were expressed as mean ± S.E. Significance in differences was tested by 1-way ANOVA, followed by Dunnett's test. Differences were considered significant when the p-value was <0.05.

3. Results

3.1. *In vitro studies*

3.1.1. *TGF-β_1 secretion and expression*

We have previously described that IFN-α2b-induced apoptosis is mediated by TGF-β_1 [4]. Here, we examined whether TGF-β_1 was synthesized and secreted by hepatocytes when treated with IFN-α2b. As shown in Fig. 1, presence of IFN-α2b in the culture media induced a twofold increase of TGF-β_1 secretion at 7 h of culture. TGF-β_1 levels in culture media continued significantly increased at 20 and 24 h of culture. When ASC was added to the culture media, TGF-β_1 levels remained unchanged.

TGF-β_1 mRNA levels increased at 4 h of IFN-α2b stimulus (Fig. 2). The presence of ASC totally abolished the increase of TGF-β_1 mRNA levels.

3.1.2. *Apoptosis*

Fig. 3 shows the time-dependent apoptotic pattern of hepatocytes. Cells treated with IFN-α2b showed a significant increase of apoptosis since 20 h of culture onwards. The other treatments completely abolished the onset of apoptosis.

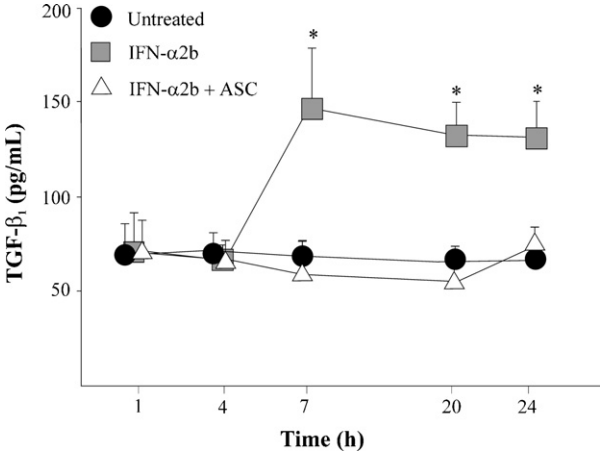

Fig. 1 – Hepatocyte TGF-β_1 secretion pattern. 1×10^6 cells were incubated at different times with IFN-α2b, IFN-α2b + ASC or left untreated. After treatment, media were collected and assayed for TGF-β_1 secretion by ELISA. Results are mean ± S.E. from at least four independent experiments. $^*p < 0.05$ vs. control (untreated) cells.

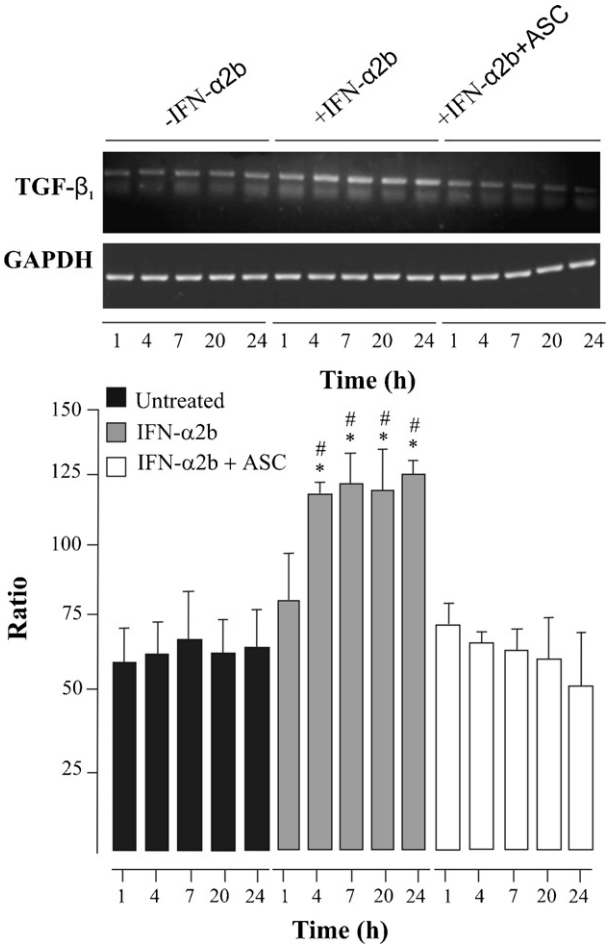

Fig. 2 – IFN-α2b-induced upregulation of TGF-β_1 mRNA. Cells were treated for different time periods with IFN-α2b, IFN-α2b + ASC or left untreated. Total RNA was isolated and TGF-β_1 and GAPDH mRNA were assessed by RT-PCR analysis. Relative mRNA levels were quantitated, and TGF-β_1 levels were normalized to GAPDH mRNA. Ratios are presented in graphical form, and the data are representative of four experiments. $^*p < 0.05$ vs. control (untreated) cells. $^\#p < 0.05$ vs. IFN-α2b-treated cells at 1 h of culture.

3.1.3. *Intracellular ROS*

ROS production induced by IFN-α2b is shown in Fig. 4. IFN-α2b-treated hepatocytes presented a peak in ROS production at 1 h of culture, and another peak at 9 h. The addition of anti-TGF-β_1 to the culture media did not block the production of the first peak of ROS whereas totally blocked the appearance of the second one. On the other hand, when ASC was added to the culture media the production of both peaks was abolished.

3.1.4. *NADPH oxidase activity*

To investigate the source of ROS, we measured the activity of NADPH oxidase enzyme. As shown in Fig. 5 after IFN-α2b treatment, NADPH oxidase was significantly activated at 1 h of

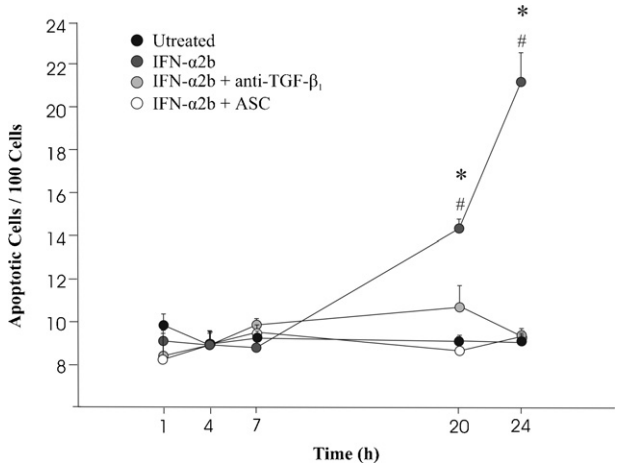

Fig. 3 – Time course analysis of the IFN-α2b-induced apoptosis. Apoptotic cells were determined by the Annexin V-FITC staining. Apoptotic cells were expressed over one hundred cells randomly counted. The results are presented as the mean ± S.E. of three independent experiments. *$p < 0.05$ vs. control cells; #$p < 0.05$ vs. IFN-α2b-treated cells at 4 h of culture.

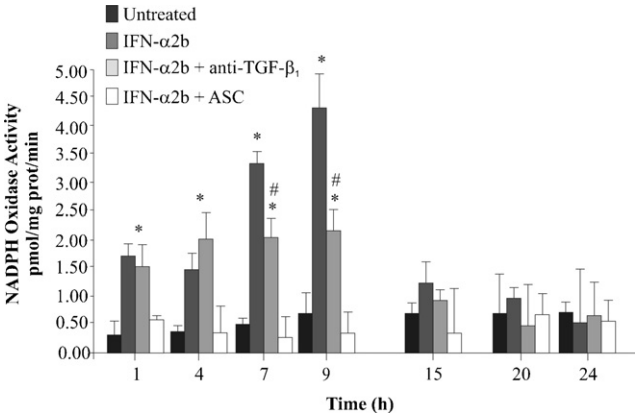

Fig. 5 – IFN-α2b-induced NADPH oxidase activity. 1×10^4 cells were incubated with IFN-α2b, IFN-α2b + anti-TGF-β_1, IFN-α2b + ASC or left untreated. NADPH consumption was monitored by decrease in absorbance at 340 nm for 10 min. For specific oxidase activity, NADPH consumption was measured by adding 10 μmol/L DPI 30 min before the assays. Results are expressed as picomoles per mg of protein per min and are the means ± S.E. of three independent experiments. *$p < 0.05$ vs. untreated cells; #$p < 0.05$ vs. IFN-α2b-treated cells.

culture, reaching a maximum at 9 h. Interestingly, addition of anti-TGF-β_1 to the culture media did not block the enzyme activation at 1 h of culture, but inhibition occurred at 9 h, reaching the same activity values that at 1 h. In all the cases, treatment with ASC totally blocked NADPH oxidase activation.

3.1.5. *GSH metabolism and antioxidant enzymes*

Fig. 6A shows that IFN-α2b treatment did not produce any variation in intracellular tGSH levels until 7 h of culture, where the levels decreased about 50%. When anti-TGF-β_1 or ASC were added to the culture media, tGSH levels remained unchanged at all the studied times. We also found that intracellular oxidized glutathione (GSSG) remained unchanged at all the studied times in all groups (data not shown). For that reason, we studied the levels of GSSG in the extracellular media. Fig. 6B shows that there was a GSSG efflux to the culture media. When cells were treated with ASC or anti-TGF-β_1, levels of GSSG in the culture media were similar to those found for the untreated cells. Then, the activity of GCL, the rate limiting enzyme of GSH synthesis, was examined. Results showed that after 7 h of IFN-α2b treatment GCL activity decreased 23% reaching a maximum decrease of 80% at 24 h of culture. At the same time, after IFN-α2b plus anti-TGF-β_1, and IFN-α2b plus ASC treatments, GCL activity remained unchanged (Fig. 7). To determine if IFN-α2b regulates the expression of the catalytic subunit of GCL (GCLC) at the transcriptional level, GCLC mRNA amounts were assessed by RT-PCR. IFN-α2b treatment resulted in a reduction in GCLC mRNA within 7 h of culture (Fig. 8A). As shown in Fig. 8B, when anti-TGF-β_1 or ASC were added, IFN-α2b treatment had no effect on the GCLC mRNA levels.

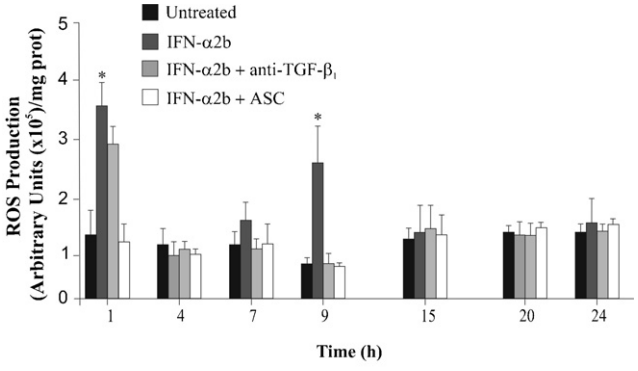

Fig. 4 – IFN-α2b induction of intracellular reactive oxygen species content. Hepatocytes from preneoplastic livers were cultured for different times in the absence or presence of IFN-α2b, IFN-α2b + anti-TGF-β_1, and IFN-α2b + ASC. Cells were loaded with 5 μM 2′,7′-dichlorofluorescin diacetate (DCFH-DA) for 20 min at 37 °C with 5% CO_2, scrapped off and fluorescence was measured. Results are expressed as arbitrary units of DCFH fluorescence/mg protein. Data are mean ± S.E. from at least four independent experiments. *$p < 0.05$ vs. control cells.

As shown in Fig. 9A, IFN-α2b induced a decrease in CAT activity from 7 h of culture and the addition of anti-TGF-β_1 or ASC totally restored the enzymatic activity to the control levels (untreated cells). Fig. 9B shows the effect of IFN-α2b in the Cu,Zn-SOD and Mn-SOD activities. Fig. 9B, upper panel, shows that Cu,Zn-SOD activity decreased from 7 h of culture in the presence of IFN-α2b. When cells were treated with anti-TGF-β_1 or ASC, the Cu,Zn-SOD activity did not change. Fig. 9B, lower panel, shows that Mn-SOD activity significantly decreased from 4 h of culture with respect to untreated cells. When anti-TGF-β_1 was added to the culture media, Mn-SOD

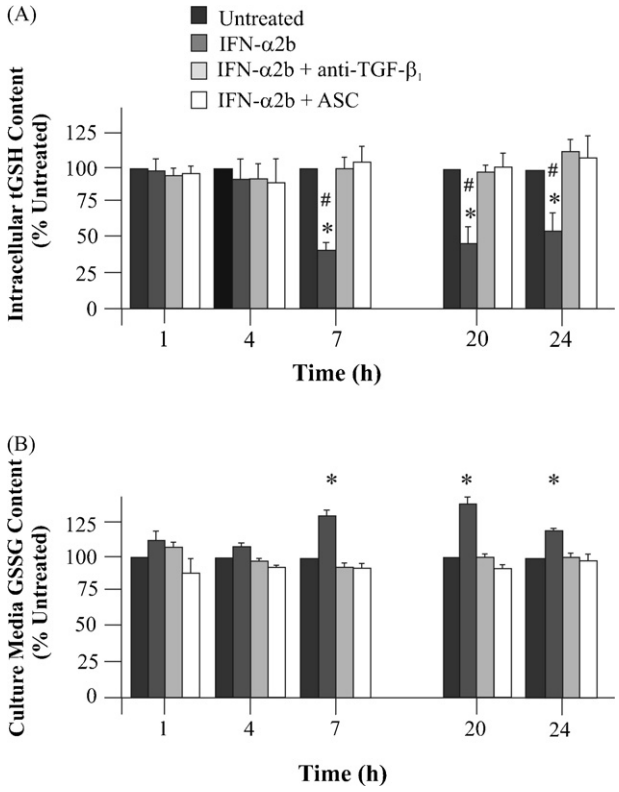

Fig. 6 – Time course analysis of the glutathione content. (A) Total cellular GSH content in cultured hepatocytes. Cells were treated with IFN-α2b, IFN-α2b + anti-TGF-β_1, IFN-α2b + ASC, or left untreated for different times. tGSH levels are reported as μg per μg protein in the initial cell extract and expressed as percentage of untreated cells. Results represent mean ± S.E. of at least five experiments. $^{*}p < 0.05$ vs. untreated cells; $^{\#}p < 0.05$ vs. IFN-α2b-treated cells at 4 h of culture. (B) Oxidized glutathione content in the culture media. GSSG levels are reported as μg per μg protein in the initial cell extract and expressed as percentage of untreated cells. Results represent mean ± S.E. of at least four experiments. $^{*}p < 0.05$ vs. untreated cells.

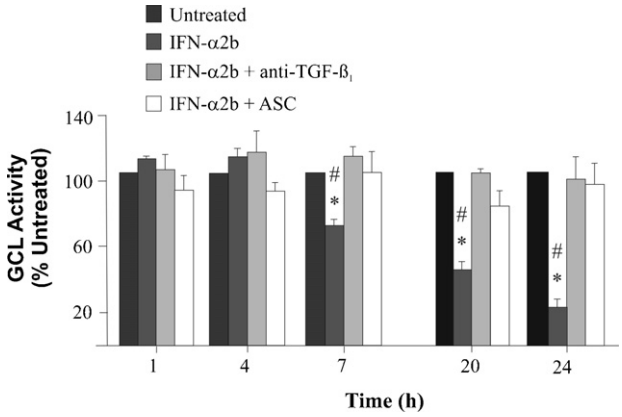

Fig. 7 – Analysis of the GCL activity. Cells were treated with IFN-α2b, IFN-α2b + anti-TGF-β_1, IFN-α2b + ASC, or left untreated at different times. Whole-cell extracts were prepared and analyzed for GCL enzymatic activity. Results are the mean ± S.E. of four experiments. $^{*}p < 0.05$ vs. untreated cells; $^{\#}p < 0.05$ vs. IFN-α2b-treated cells at 4 h of culture.

activity reached the same values of untreated cells at 7 h of culture. Treatment with ASC totally abolished the enzyme activity decrease at all the studied times.

3.2. *In vivo studies*

3.2.1. *rGST P-positive cells analysis*

Changes in number and volume percentage of the liver of rGST P-positive foci are shown in Fig. 10. The number and volume percentages of AHF per liver in the rats given IFN-α2b were significantly decreased as compared with the values from the IP group. IFN-α2b treatment reduced 80% the total number of initiated cells capable of developing into clones of AHF respect to IP group. In IP + IFN-α2b + ASC group, and IP + ASC group no differences in the number of AHF were observed with respect to IP group. IFN-α2b decreased the growth rate and total cellular population of AHF, measured as the volume fraction of the liver occupied by foci (34% in the IFN-α2b treated rats with respect to control). No differences were observed between the IP + ASC treated group and the IP group. Interestingly, foci volume was 94% higher in the IP + IFN-α2b + ASC group than in IP + IFN-α2b.

3.2.2. *PI and AI analysis*

PI and AI data are summarized in Table 2.

PI in AHF was significantly increased compared with their respective surrounding tissue in all the studied groups, but it was not significant among the different groups. There was no difference in the AI of AHF compared with their respective surrounding tissue. However, AI in AHF of IP + IFN-α2b-treated rats showed a significant increment as compared with groups IP, IP + ASC and IP + IFN-α2b + ASC. Apoptotic cells were seen in hematoxylin/eosin stained liver sections of all groups and no pathological evidence of necrosis was observed. Incidence of apoptotic cells in hematoxylin/eosin stained sections revealed almost the same values and tendencies as the obtained in TUNEL stained sections (data not shown).

4. Discussion

The earliest emerging types of AHF are composed of differentiated hepatocytes that show characteristic metabolic and molecular aberrations and gradually progress via various intermediate forms to the poorly differentiated neoplastic phenotype [25]. In a previous work, we showed that administration of IFN-α2b decreased both number and volume percentage of the placental form of rGST-positive preneoplastic foci through an apoptotic mechanism [3]. We have also demonstrated that IFN-α2b induces apoptosis in isolated hepatocytes from rat preneoplastic livers via TGF-β_1 secretion and, in contrast to these hepatocytes, normal rat hepatocytes did not respond to IFN-α2b treatment inducing neither TGF-β_1

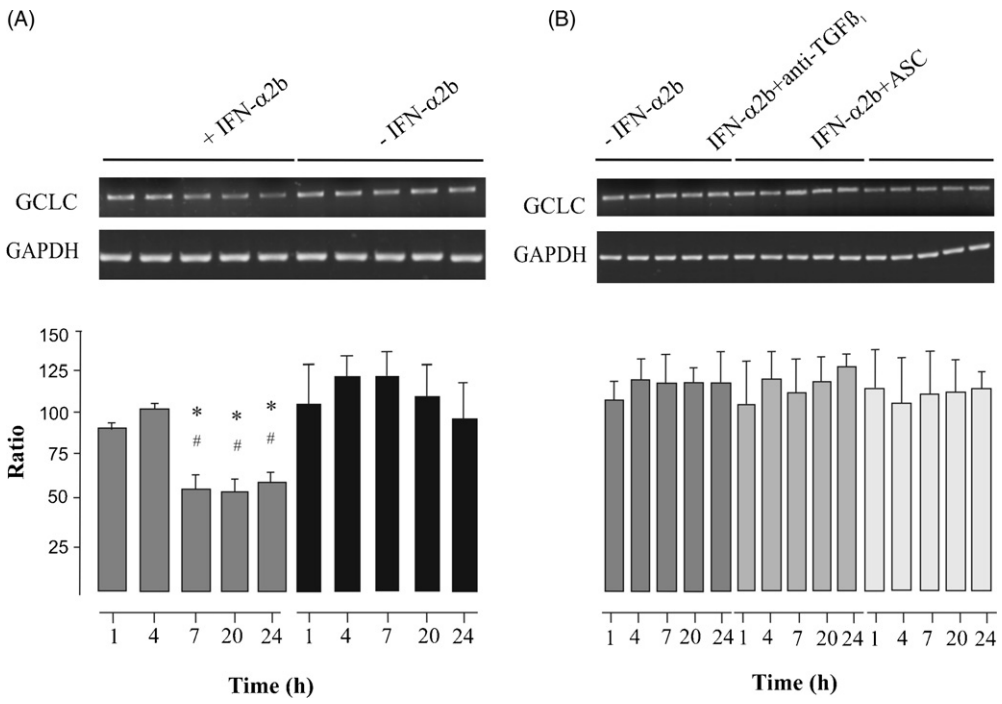

Fig. 8 – IFN-α2b-induced downregulation of GCLC. Cells were treated at different times with (A) IFN-α2b or left untreated and (B) IFN-α2b plus anti-TGF-β_1, IFN-α2b plus ASC or left untreated. Total RNA was isolated and GCLC and GAPDH mRNA were assessed by RT-PCR analysis. Relative mRNA levels were quantitated, and GCLC levels were normalized to GAPDH mRNA. Ratios are presented in graphical form, and the data are representative of four experiments. *$p < 0.05$ vs. untreated cells. #$p < 0.05$ vs. IFN-α2b-treated cells at 4 h of culture.

secretion nor apoptosis [4]. In the current series of experiments, we proved that IFN-α2b induces the production of TGF-β_1 in hepatocytes from preneoplastic livers by activation of NADPH oxidase complex, and TGF-β_1 induces apoptosis through a mechanism linked to the production of ROS by the same oxidase. In order to confirm that the induction of NADPH oxidase activity was the main pathway producing ROS, additional experiments were made using IFN-α2b plus an inhibitor of NADPH oxidase activity, DPI. Presence of DPI in the culture media totally blocked the activity of NADPH oxidase, the production of ROS and the subsequent apoptosis induced by IFN-α2b (results not shown).

Results from the *in vitro* studies showed that IFN-α2b treatment of hepatocytes obtained from rat preneoplastic livers induces secretion of TGF-β_1 to the culture media and this secretion is accompanied by an increase in the mRNA levels of the cytokine. This increase is linked with the presence of ROS in the intracellular media. ROS production could be totally blocked when a scavenger such as ASC was added to the culture media, and thus, the IFN-α2b-induced apoptotic effect was totally abolished. It is known that IFN-γ activates the phagocytic NADPH oxidase to produce superoxide radical against pathogenic bacteria [26] and upregulates the production of superoxide anion by NADPH oxidase in human intestinal epithelial cells [27]. However, little is known about the relationship between IFN-α, activation of NADPH oxidase, and epithelial cells. It has been reported that IFN-α2b enhances the NADPH oxidase activity in human neutrophils [28]. In hepatocytes treated with hydrophobic bile salts, an enhancement of a membrane NADPH oxidase activity triggering ROS formation was also shown [29]. Although further investigation on the isoforms of the NADPH oxidase complex is needed, we are demonstrating for the first time that IFN-α2b induces an early activation of this enzyme complex in hepatocytes obtained from rat preneoplastic liver. Results lead us to conclude that IFN-α2b induces the early ROS production that serves as a messenger, promoting the TGF-β_1 production and secretion. This growth factor triggers the production of more reactive oxygen intermediates, as a late event, by inducing the same enzyme complex. It was demonstrated that synthesis of a new protein is required for NADPH activation and subsequent apoptosis [7]. This event shows an additive response in ROS production and imposes the final onset of the apoptotic effect. The presence of ASC in the culture media totally blocked the increase in the activity of the NADPH oxidase complex at all the studied times. These results are in agreement with other authors that demonstrated that the activity of this complex is lowered by the presence of antioxidants such as ASC or vitamin E in several cell types [30–32].

Once the source of ROS was assessed, we analyzed the cellular antioxidant defenses and their behavior during the incubation times. We observed a reduction in tGSH levels from 7 h of culture onwards. For that reason we studied if any form of glutathione was being exported out of the cell, and whether the biosynthetic GSH capacity was altered. We found an increase in GSSG levels probably due to the oxidation of the reduced form within the cytosol, and its exportation to the

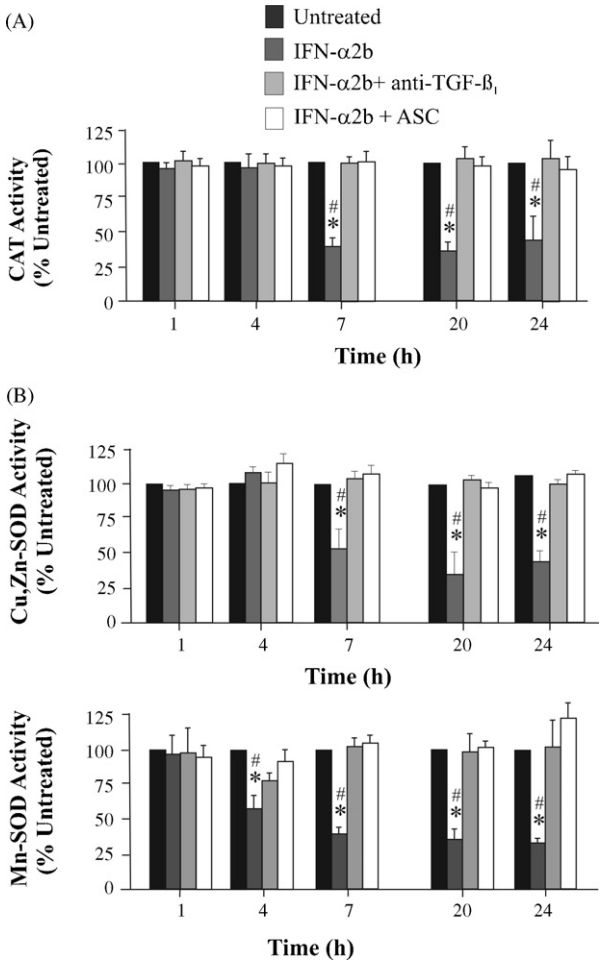

Fig. 9 – Time course analysis of the effect of IFN-α2b on enzymatic activities of CAT and SOD. Cell were left untreated (control) or incubated with IFN-α2b, IFN-α 2b + anti-TGF-β_1 and IFN-α2b + ASC. (A) CAT enzymatic activity was determined by monitoring the rate of decomposition of H_2O_2, as a function of the decrease in absorbance at 240nm. (B) SOD activity was assayed by inhibition of nitrite formation from hydroxylammonium in the presence of superoxide anion generators. In all cases results are expressed as percentages of control and are the mean ± S.E. of four independent experiments. *$p < 0.05$ vs. control cells; IFN-α2b-treated cells at 4 h of culture.

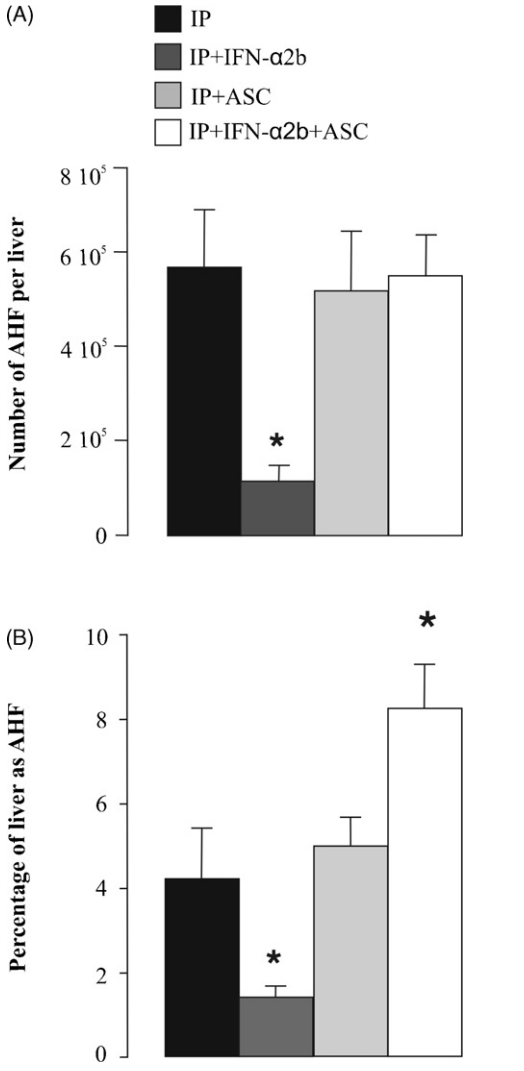

Fig. 10 – Changes in (A) number of AHF per liver and (B) percentage of liver as AHF. AHF were visualized with rGST-P staining, and treatment groups are indicated as different color bars. Each bar indicates mean ± S.E. of 8–10 animals. *$p < 0.05$ vs. IP group.

culture media, possibly in order to protect the cell from a shift in the redox equilibrium. IFN-α2b treatment resulted in the loss of GSH biosynthetic capacity since GCL activity was decreased at 7 h of culture and a rapid decrease of GCLC mRNA expression through a mechanism mediated by TGF-β_1 was also observed. Moreover, it was found that IFN-α2b-induced apoptosis in hepatocytes from rat preneoplastic livers is accompanied by the cleavage and loss of GCLC protein, through a mechanism mediated by TGF-β_1 (data not shown).

A decrease in CAT and SOD activities was observed when hepatocytes were treated with IFN-α2b. On the other hand, treatment with anti-TGF-β_1 or ASC totally blocked the decrease in CAT and SOD enzymatic activities. These findings indicate that IFN-α2b induced the decrease in enzymatic CAT and SOD activities by a mechanism mediated by ROS and TGF-β_1. These enzymes probably protect hepatocytes from the initial IFN-α2b-induced burst of ROS and this may be the reason for the rapid decrease of the first peak of ROS. Moreover, the decrease in CAT and SOD activities would further exacerbate the existing oxidative stress. These results confirmed that the perturbation of the redox status produced by the IFN-α2b induction of NADPH oxidase complex triggered TGF-β_1 synthesis and secretion and assessed the down-regulation of antioxidative systems. Similar data have been reported by Herrera et al. [7] when they treated fetal rat hepatocytes with TGF-β_1.

Since ASC abolished all the apoptotic effects induced *in vitro* by IFN-α2b, we determined the relevance of ROS on the onset of the apoptotic process *in vivo* in the whole preneo-

Table 2 – PI and AI in AHF and their surrounding tissue

	IP	IP + IFN-α2b	IP + ASC	IP + IFN-α2b + ASC
PI				
AHF	$21.55 \pm 1.25^{\#}$	$21.00 \pm 1.00^{\#}$	$20.75 \pm 1.11^{\#}$	$21.75 \pm 1.20^{\#}$
Surrounding tissue	3.8 ± 0.1	3.9 ± 0.4	4.1 ± 0.2	4.3 ± 0.3
AI				
AHF	0.21 ± 0.01	$0.38 \pm 0.06^{*}$	0.21 ± 0.04	0.19 ± 0.03
Surrounding tissue	0.10 ± 0.01	0.14 ± 0.05	0.12 ± 0.05	0.08 ± 0.02

Note: PI was expressed as proliferating cells per 1000 hepatocytes. $^{\#}p < 0.05$ vs. PI in their respective surrounding tissue. AI was expressed as apoptotic cells scored per 100 hepatocytes. $^{*}p < 0.05$ vs. AI in group IP.

plastic liver. Treatment of IP rats with IFN-α2b + ASC abolished the IFN-α2b apoptotic effects observed in the IFN-α2b-treated rats. The relationship between proliferation and apoptosis rates, which determines the foci volume in IP + IFN-α2b rats, might be modified by the presence of ASC, probably diminishing the apoptotic rate. Although there were no differences in AI, it was observed a non statistically decrease trend in IP + IFN-α2b + ASC group and this could be the reason for the increase of foci volume in this group. Besides, it was found that ASC at low concentrations stimulates growth of malignant cells [33], while inhibits their growth at high doses [34]. At the present time, many cancer patients combine some forms of complementary and alternative medicine therapies with their conventional therapies. The most common choice of these therapies is the use of antioxidants such as vitamin C. It must be assumed that any antioxidant, used to reduce toxicity of tumor therapy on healthy tissue, has the potential to decrease effectiveness of cancer therapy on malignant cells [35]. Some data suggest that antioxidants can ameliorate toxic side effects of therapy without affecting treatment efficacy, whereas other data suggest that antioxidants interfere with radiotherapy or chemotherapy [35].

In conclusion, in this work, we demonstrated that increase in ROS levels turns on the process of programmed hepatocytes death, leading to the elimination of these malignant cells. ROS were viewed as the ''bad'' molecules of cells for a long time, but in the recent years, several lines of evidence indicate the contrary: ROS are essential participants in cell signaling and regulation [36,37] depending on its concentration. On the other hand, the inhibition of ROS production with an antioxidant such as ASC in the co-treatment with IFN-α2b may be not a beneficial therapy for the prevention of AHF appearance. Furthermore, IFN-α2b + ASC co-treatment enhances the volume of the preneoplastic foci. This constitutes a very important contribution in terms of understanding ASC effect on malignant cells. In addition, this and other studies, instead of being contradictory, help to determine a therapeutic dosing range of ASC on cancer, specifically, the proper dose and the concomitant use of therapeutic drugs such as IFN-α2b.

Acknowledgements

The authors express their gratitude to Bio Sidus S.A. for the generous gift of recombinant IFN-α2b (BIOFERON) and to Dr. Enrique Sánchez Pozzi for his expert computational assistance and his critical reading and helpful suggestions. We also thank Justina E. Ochoa, Juan A. Monti, and María C. Lugano for their helpful experimental assistance. This work was supported by Research Grant PICT 05-11107 (MC Carrillo) from Agencia Nacional de Promoción Científica y Tecnológica (ANPCyT) and by Consejo Nacional de Investigaciones Científicas y Técnicas (CONICET, PIP No. 6349) (MC Carrillo).

REFERENCES

[1] Yano H, Iemura A, Haramaski M, Ogasawara S, Takayama A, Akiba J, et al. Interferon alfa receptor expression and growth inhibition by interferon alfa in human cancer cell lines. Hepatology 1999;29:1708–17.
[2] Murphy D, Detjen KM, Welzel M, Wiedenmann B, Rosewicz S. Interferon-α delays S-phase progression in human hepatocellular carcinoma cells via inhibition of specific cyclin-dependent kinases. Hepatology 2001;33: 346–56.
[3] de Lujan Alvarez M, Cerliani JP, Monti J, Carnovale C, Ronco MT, Pisani G, et al. The *in vivo* apoptotic effect of interferon alfa-2b on rat preneoplastic liver involves Bax protein. Hepatology 2002;35:824–33.
[4] de Lujan Alvarez M, Ronco MT, Ochoa JE, Monti J, Carnovale C, Pisani G, et al. IFN-α-induced apoptosis on rat preneoplastic liver is mediated by hepatocytic transforming growth factor-β_1. Hepatology 2004;40:394–402.
[5] Herrera B, Alvarez AM, Sanchez A, Fernandez M, Roncero C, Benito M, et al. Reactive oxygen species (ROS) mediates the mitochondrial-dependent apoptosis induced by transforming growth factor β in fetal hepatocytes. FASEB J 2001;15:741–51.
[6] Franklin C, Rosenfeld-Franklin M, White C, Kavanagh T, Fausto N. TGF-β_1-induced suppression of glutathione antioxidants defenses in hepatocytes: caspase-dependent posttranslational and caspase-independent transcriptional regulatory mechanisms. FASEB J 2003;17:1535–7.
[7] Herrera B, Murillo MM, Álvarez-Barrientos A, Beltrán J, Fernández M, Fabregat I. Source of early reactive oxygen species in the apoptosis induced by transforming growth factor-β in fetal rat hepatocytes. Free Radic Biol Med 2004;36:16–26.
[8] Babior BM. The NADPH oxidase of endothelial cells. IUBMB Life 2000;50:267–9.
[9] Mizukami Y, Matsubara F, Matsukawa S, Izumi R. Cytochemical localization of glutaraldehyde-resistant NAD(P)H-oxidase in rat hepatocytes. Histochemistry 1983;79:259–67.
[10] Coyle B, Freathy C, Grant TW, Roberts RA, Cain K. Characterization of the transforming growth factor-β_1-induced apoptotic transcriptome in FaO hepatoma cells. J Biol Chem 2003;278:5920–8.
[11] Ronco MT, Alvarez ML, Monti JA, Carrillo MC, Pisani G, Lugano C, et al. Modulation of balance between apoptosis

and proliferation by lipid peroxidation during rat liver regeneration. Mol Med 2002;8(12):807–16.
[12] Seglen PO. Preparation of rat livers cells. 3. Enzymatic requirement for tissue dispersion. Exp Cell Res 1973;82:391–8.
[13] LeBel CP, Ischiropoulos H, Bondy SC. Evaluation of the probe 2′,7′-dichlorofluorescin as an indicator of reactive oxygen species formation and oxidative stress. Chem Res Toxicol 1992;5:227–31.
[14] Baker MA, Cerniglia GJ, Zaman A. Microtiter plate assay for the measurement of glutathione and glutathione disulfide in large number of biological samples. Anal Biochem 1990;190:360–5.
[15] Seelig GF, Simondsen RP, Meister A. Reversible dissociation of γ-glutamylcysteine synthetase into two subunits. J Biol Chem 1984;259:9345–7.
[16] Carrillo MC, Kitani K, Kanai S, Sato Y, Miyasaka K, Ivy GO. (−)deprenyl increases activities of superoxide dismutase and catalase in certain brain regions in old male mice. Life Sci 1994;54:975–81.
[17] Elstner EF, Heupel A. Inhibition of nitrite formation from hydroxylamonium-chloride: a simple assay for superoxide dismutase. Anal Bichem 1976;70:616–20.
[18] Lowry OH, Rosembrough NJ, Farr AL, Randall RJ. Protein measurements with the Folin-phenol reagent. J Biol Chem 1951;193:265–75.
[19] Kaku T, Ekem K, Lindayen C, Bailey DJ, van Nostrand AWP, Farber E. Comparison of formalin- and acetone-fixation for immunohistochemical detection of carcioembryogenic antigen (CEA) and keratin. Am J Clin Pathol 1983;80:806–15.
[20] Imai T, Masui T, Ichinose M, Nakanishi H, Tokuma Y, Masegi T, et al. Reduction of glutathione S-transferase P-form mRNA expression in remodeling nodules in rat liver revealed by *in situ* hybridization. Carcinogenesis 1997;18:545–51.
[21] Pitot H. Altered hepatic foci: their role in murine hepatocarcinogenesis. Annu Rev Pharmacol Toxicol 1990;30:465–500.
[22] Saltykov SA. The determination of the size distribution of particles in an opaque material for measurement of the size distribution of their sections. In: Elias H, editor. Proceedings of the Second International Congress for Stereology. Berlin: Springer-Verlag; 1967. p. 163–73.
[23] Greenwell A, Foley JF, Maronpot RR. An enhancement method for immunohistochemical staining of proliferating cell nuclear antigen in archival rodent tissues. Cancer Lett 1991;59:251–6.
[24] Gold R, Schmied M, Giegerich G, Breitschopf H, Hartung HP, Toyka KV, et al. Differentiation between cellular apoptosis and necrosis by the combined use of *in situ* tailing and nick translation techniques. Lab Invest 1994;71:219–25.
[25] Bannasch P, Haertel T, Su Q. Significance of hepatic preneoplasia in risk identification and early detection of neoplasia. Toxicol Pathol 2003;31:134–9.
[26] Babior BM, Kipnes RS, Curnutte JT. Biological defense mechanisms. The production by leukocytes of superoxide, a potential bactericidal agent. J Clin Invest 1973;52:741–4.
[27] Kuwano Y, Kawahara T, Yamamoto H, Teshima-Kondo S, Tominaga K, Masuda K, et al. Interferon-γ activates transcription of NADPH oxidase 1 gene and upregulates production of superoxide anion by human large intestinal epithelial cells. Am J Physiol Cell Physiol 2005;290:C433–43.
[28] Koie T, Suzuki K, Kudo S, Yamada M, Liu Q, Nakaji S, et al. The effects of interferon-alpha on oxygen radical production by human neutrophils. Nippon Eiseigaku Zasshi 1998;53:536–44.
[29] Reinehr R, Becker S, Keitel V, Eberle A, Grether-Beck S, Haussinger D. Bile salt-induced apoptosis involves NADPH oxidase isoform activation. Gastroenterology 2005;129:2009–31.
[30] Ulker S, McMaster D, McKeown PP, Bayraktutan U. Antioxidant vitamins C and E ameliorate hyperglycaemia-induced oxidative stress in coronary endothelial cells. Diabetes Obes Metab 2004;6:442–51.
[31] Chade AR, Bentley MD, Zhu X, Rodriguez-Porcel M, Niemeyer S, Amores-Arriaga B, et al. Antioxidant intervention prevents renal neovascularization in hypercholesterolemic pigs. J Am Soc Nephrol 2004;15:1816–25.
[32] Zhan CD, Sindhu RK, Vaziri ND. Up-regulation of kidney NAD(P)H oxidase and calcineurin in SHR: reversal by lifelong antioxidant supplementation. Kidney Int 2004;65:219–27.
[33] Park CH. Vitamin C and leukemia and proleukemia cell growth. Prog Clin Biol Res 1998;259:321–30.
[34] Prasad KN, Kumar R. Effect of individual and multiple antioxidant vitamins on growth and morphology of human non-tumorogenic and tumorogenic parotid acinar cell in cultures. Nutr Cancer 1996;18:2487–93.
[35] Seifried HE, McDonald SS, Anderson DE, Greenwald P, Milner JA. The antioxidant conundrum in cancer. Cancer Res 2003;63:4295–8.
[36] Rhee SG. Redox Signalling: hydrogen peroxide as intracellular messenger. Exp Mol Med 1999;31:53–9.
[37] Finkel T. Oxygen radicals and signaling. Curr Opin Cell Biol 1998;10:248–53.